J Korean Med Sci 2009; 24: 1089-98
ISSN 1011-8934
DOI: 10.3346/jkms.2009.24.6.1089

Inhibition of the Human *Ether-a-go-go*-related Gene (HERG) K^+ Channels by *Lindera erythrocarpa*

Lindera erythrocarpa Makino (Lauraceae) is used as a traditional medicine for analgesic, antidote, and antibacterial purposes and shows anti-tumor activity. We studied the effects of *Lindera erythrocarpa* on the human *ether-a-go-go*-related gene (*HERG*) channel, which appears of importance in favoring cancer progression in vivo and determining cardiac action potential duration. Application of MeOH extract of *Lindera erythrocarpa* showed a dose-dependent decrease in the amplitudes of the outward currents measured at the end of the pulse (I_{HERG}) and the tail currents of HERG (I_{tail}). When the BuOH fraction and H_2O fraction of *Lindera erythrocarpa* were added to the perfusate, both I_{HERG} and I_{tail} were suppressed, while the hexane fraction, $CHCl_3$ fraction, and EtOAc fraction did not inhibit either I_{HERG} or I_{tail}. The potential required for half-maximal activation caused by EtOAc fraction, BuOH fraction, and H_2O fraction shifted significantly. The BuOH fraction and H_2O fraction (100 μg/mL) decreased g_{max} by 59.6% and 52.9%, respectively. The H_2O fraction- and BuOH fraction-induced blockades of I_{tail} progressively decreased with increasing depolarization, showing the voltage-dependent block. Our findings suggest that *Lindera erythrocarpa*, a traditional medicine, blocks HERG channel, which could contribute to its anticancer and cardiac arrhythmogenic effect.

Key Words : *Anti-Tumor Activity; Arrhythmias, Cardiac; HERG Channel; I_{Kr}; Lindera erythrocarpa*

Hee-Kyung Hong[1,*], Weon-Jong Yoon[2,*], Young Ho Kim[3], Eun-Sook Yoo[2], and Su-Hyun Jo[1]

Department of Physiology[1], Institute of Bioscience and Biotechnology, Kangwon National University College of Medicine, Chuncheon; Department of Pharmacology[2], Cheju National University College of Medicine, Jeju; College of Pharmacy[3], Chungnam National University, Daejeon, Korea

*These authors contributed equally to this work.

Received : 9 June 2008
Accepted : 3 December 2008

Address for correspondence
Su-Hyun Jo, Ph.D.
Department of Physiology, Kangwon National University College of Medicine, Hyoja-dong, Chuncheon 200-701, Korea
Tel : +82.33-250-8824, Fax : +82.33-255-8809
E-mail : suhyunjo@kangwon.ac.kr

This work was supported by the research grant of the Cheju National University in 2006.

INTRODUCTION

Lindera erythrocarpa Makino (*L. erythrocarpa*) belongs to the large family Lauraceae, which consists mostly of trees or shrubs from the warmer regions of the earth. It is distributed throughout Korea, China, and Japan (1). *Lindera* species, including *L. lucida*, *L. strychnifolia*, *L. aggregate* and *L. chunii* are important medicinal plants. The fruit of *L. erythrocarpa* is used as a traditional medicine for analgesic, digestive, diuretic, antidote, and antibacterial purposes; also, its leaves have been used as a folk medicine for stomach-ache, thirst, and neuralgia (1-3). Cyclopentenediones, farnesyl protein transferase inhibitors, and anti-tumor compounds were isolated from the methanolic extract of the fruits of *L. erythrocarpa* (4). These compounds strongly inhibit human colon tumor cells and exert their anti-tumor activity by inducing apoptosis through the caspase-3 pathway (4). Also, three lignans isolated from a methanol extract of *L. erythrocarpa* were evaluated for in vitro cytotoxicity using three cancer cell line assays, and among these compounds, methyllinderone showed significant cytotoxicity against mouse melanoma, human acetabulum fibrosarcoma, and myelogenous leukemia cell lines (5).

The rapid component of a cardiac delayed rectifier potassium current (I_{Kr}) is known to play a critical role in repolarization of action potential (6). I_{Kr} is one of the targets for antiarrhythmic therapy, since the blocking of this current is expected to increase the action potential duration (APD) and thereby increase the refractory period (7). It has been shown that the human *ether-a-go-go*-related gene (*HERG*) encodes a major component of the I_{Kr} and that congenital mutation of HERG results in long QT syndrome, which shows a high risk of sudden death due to torsade de pointes type ventricular arrhythmia (8). While HERG K^+ channels control electrical activity in excitable cells, these channels are also significantly expressed in non-excitable cells. High levels of HERG mRNA are detected in various cancer cells (9-10), and the overexpression of *ether-a-go-go* gene (*EAG*) channels enhances aggressive growth of tumors (11). Moreover, E-4031, a specific HERG channel blocker, reduced proliferation of uterine cancer cells (12). Therefore, the cytotoxic effect of *L. erythrocarpa* for the cancer cell lines could be caused by the modulation of HERG K^+ channels (5).

In the present study, we have investigated the effect of extracts of *L. erythrocarpa* on the HERG current, a molecular equivalent of I_{Kr}, using the *Xenopus* oocyte expression system. We found that *L. erythrocarpa* blocked the HERG channel,

resulting in a shift in voltage-dependence of channel activation and reduction of maximum conductance (g_{max}). We have also examined the HERG-blocking effects of several fractions of *L. erythrocarpa*, and the H_2O and BuOH fractions exhibited the strongest changes in $V_{1/2}$ (the potential required for half-maximal activation) and g_{max} (maximum conductance) among the solvent fractions.

MATERIALS AND METHODS

Preparation of extract from *L. erythrocarpa*

The leaves of *L. erythrocarpa* were collected in October 2005 at Jeju Island, Korea. The samples were cleaned, dried at room temperature for two weeks, and ground into a fine powder. The dried materials (100 g) were extracted with 80% methanol (MeOH) at room temperature for 24 hr and then concentrated under a vacuum. The resulting MeOH extract (32 g) was suspended in water (1 L) and successively partitioned with hexane (1 L × 3), chloroform ($CHCl_3$; 1 L × 3) ethyl acetate (EtOAc; 1 L × 3), and n-butanol (BuOH; 1 L × 3), to give hexane (0.9892 g), $CHCl_3$ (1.6209 g), EtOAc (3.0058 g), BuOH (6.8221 g) and H_2O (18.5571 g) fractions, respectively.

Expression of *HERG* in oocytes

Complementary *HERG* (accession no. U04270) RNA was synthesized by in vitro transcription from 1 μg of linearized cDNA using T7 message machine kits (Ambion, Austin, TX, U.S.A.) and stored in 10 mM Tris-HCl (pH 7.4) at -80°C. Stage V-VI oocytes were surgically removed from female *Xenopus laevis* (Nasco, Modesto, CA, U.S.A.) that was anesthetized with 0.17% tricane methanesulphonate (Sigma Chemicals, St. Louis, MO, U.S.A.). Using fine forceps, theca and follicle layers were manually removed from oocytes, which were injected with 40 nL of cRNA (0.1-0.5 μg/μL). The injected oocytes were maintained in modified Barth's solution containing 88 mM NaCl, 1 mM KCl, 0.4 mM $CaCl_2$, 0.33 mM $Ca(NO_3)_2$, 1 mM $MgSO_4$, 2.4 mM $NaHCO_3$, 10 mM HEPES (pH 7.4), and 50 μg/mL gentamicin sulphonate. Currents were studied two to seven days after injection.

Solutions and voltage clamp recording from oocytes

Normal Ringer's solution contained 96 mM NaCl, 2 mM KCl, 1.8 mM $CaCl_2$, 1 mM $MgCl_2$, and 10 mM HEPES (pH adjusted to 7.4 with NaOH). All salts were purchased from Sigma Chemicals. The effects of the MeOH extract and solvent fractions on the HERG current were observed by adding 100 mg/mL stock solution of either MeOH extract or solvent fractions to the external solutions at suitable concentrations (0.01-300 μg/mL) shortly before each experiment. None of the final concentrations from any of the solvents exceeded 0.1%. Solutions were applied to the oocytes by continuous perfusion of the chamber while recording. Solution exchanges were completed within 3 min, and the HERG current was recorded after 5 min when the solution exchange was completed. The effects of several concentrations of MeOH extract, BuOH fraction, and H_2O fraction on the HERG currents were determined after the currents showed reversibility when washed with normal Ringer's solution. It took about 10 min to wash out ≤30 μg/mL MeOH extract or BuOH and H_2O fractions, and about 20 min to wash out ≥50 μg/mL. In experiments with 50-100 μg/mL BuOH and H_2O fractions, HERG currents usually (~80% of cells examined) showed >90% recovery after 20 min washing with normal Ringer's solution. If the oocyte did not recover current after 30 min of washing with normal Ringer's solution, it was not used further. Currents were measured at room temperature (21-23°C) with a two-microelectrode voltage clamp amplifier (Warner Instruments, Hamden, CT, U.S.A.). Electrodes were filled with 3 M KCl and had a resistance of 2-4 MΩ for voltage-recording electrodes and 0.6-1 MΩ for current-passing electrodes. Stimulation and data acquisition were controlled with Digidata and pCLAMP software (Axon Instruments, Sunnyvale, CA, U.S.A.).

Statistical evaluations

All data are expressed as mean ± SE. The statistical significance was analyzed by one-way ANOVA and the LSD post-hoc test was used to evaluate between groups. Resulting *P* values less than 0.05 were regarded as significant.

RESULTS

Effect of *L. erythrocarpa* on HERG K^+ currents expressed in *Xenopus* oocyte

We assayed the effects of MeOH extract and solvent fractions of *L. erythrocarpa* on HERG current using a *Xenopus* oocyte expression system. Throughout the experiments, the holding potential was held at -70 mV, and the repolarization potential was constantly held at -60 mV for the analysis of tail currents (I_{tail}). Fig. 1A shows an example of a voltage-clamp recording from a *Xenopus* oocyte and representative current traces for control conditions and after exposure to 100 μg/mL MeOH extract of *L. erythrocarpa*. Under control conditions, depolarizing steps activated time-dependent outward currents. The amplitude of the outward currents measured at the end of the pulse (I_{HERG}) increased with more positive voltage steps, reaching a maximum value at 0 mV. Depolarizing steps to even more positive values caused a current decrease, resulting in a negative slope of the I-V curve (Fig. 1B). Current-voltage relationships for I_{HERG} obtained at various concentrations

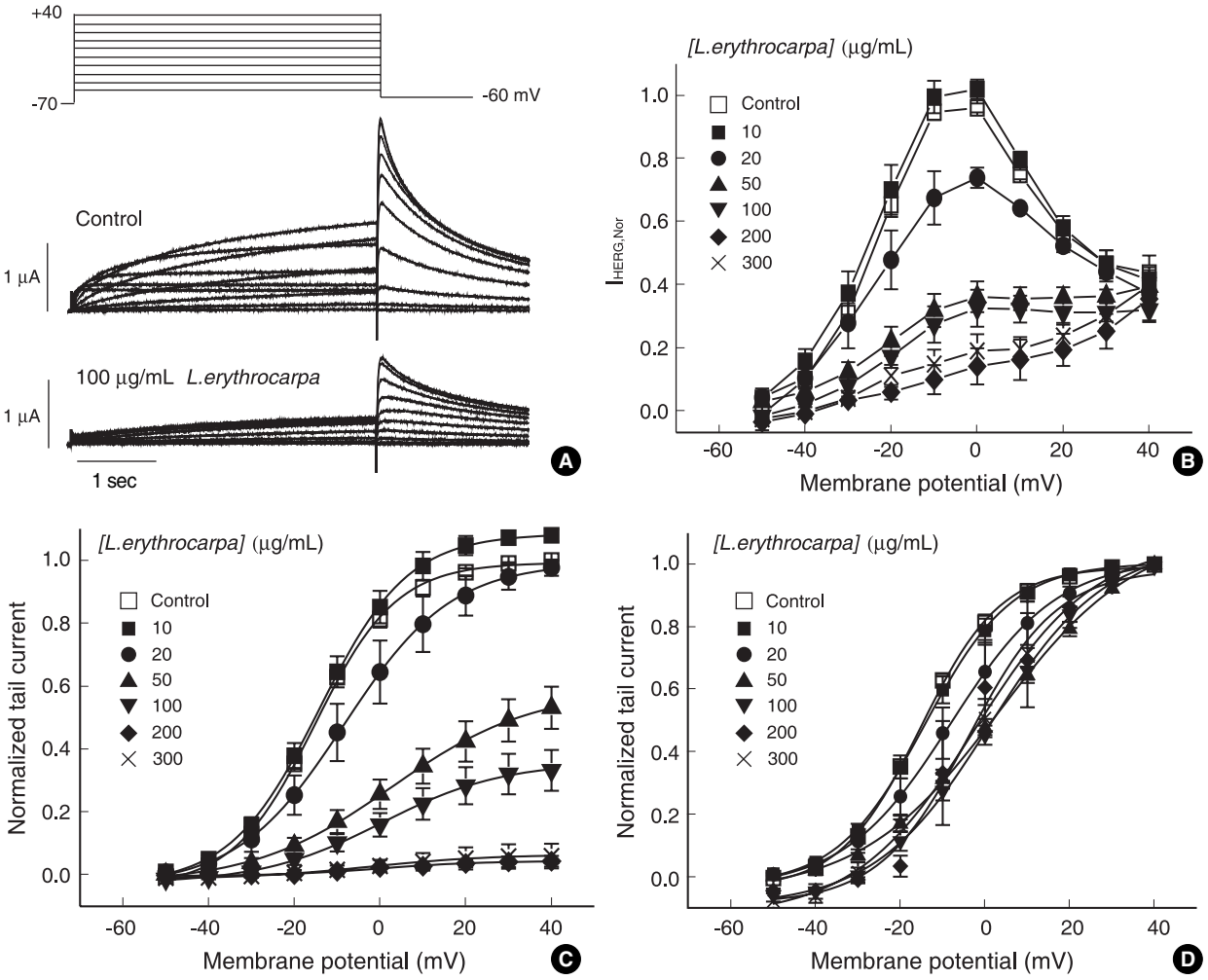

Fig. 1. Effect of *Lindera erythrocarpa* on human-*ether-a-go-go*-related-gene (HERG) currents elicited by depolarizing voltage pulses. (**A**) Superimposed current traces elicited by depolarizing voltage pulses (4 sec) in 10 mV steps (upper panel) from a holding potential of -70 mV in the absence of *L. erythrocarpa* extract (control, middle panel) and in the presence of 100 μg/mL *L. erythrocarpa* extract (lower panel). (**B**) Plot of the HERG current (I_{HERG}) measured at the end of depolarizing pulses against the pulse potential in different concentrations of *L. erythrocarpa* extract (obtained from **A**). (**C**) Plot of the normalized tail current measured at its peak just after repolarization. The amplitude of the tail current in the absence of *L. erythrocarpa* extract was taken as one. Control data were fitted to the Boltzmann equation, $y=1/\{1+\exp[(-V+V_{1/2})/dx]\}$, with $V_{1/2}$ of -15.2 mV. (**D**) Activation curves with values normalized to the respective maximum value at each concentration of *L. erythrocarpa* extract. Symbols with error bars represent means ± SEM (n=8).

of *L. erythrocarpa* extract are plotted in Fig. 1B. As the concentration of the extract progressively increased, the amplitude of I_{HERG} showed a dose-dependent decrease.

After the depolarizing steps, repolarization to -60 mV induced outward I_{tail}, which had an amplitude even larger than that of I_{HERG} during depolarization. This is a characteristic property of HERG currents, which is due to rapid recovery from inactivation and a slow deactivation mechanism (13). The amplitude of I_{tail} increased with depolarizing steps from -50 to +20 mV, and was then superimposed on further depolarizing steps to +40 mV. When 100 μg/mL MeOH extract of *L. erythrocarpa* was added to the perfusate, both I_{HERG} and I_{tail} were suppressed (Fig. 1A, bottom panel). The amplitude of I_{tail} was normalized to the peak amplitude obtained under control conditions at maximum depolarization and was plotted against the potential of the step depolarization (Fig. 1C). The normalized I_{tail} reflects a voltage-dependent activation of the HERG channels. Data obtained under control conditions were well fitted by the Boltzmann equation, with half-maximal activation ($V_{1/2}$) at -15.2 mV. As the concentration of the MeOH extract of *L. erythrocarpa* was increased, the peak I_{tail} amplitude decreased, indicating that the g_{max} of HERG channels is decreased by *L. erythrocarpa*.

Voltage-dependent HERG channel blockade by *L. erythrocarpa*

For further analysis, we normalized the values in Fig. 1C to

the respective maximum value at each concentration to examine a possible activation curve shift induced by the MeOH extract of *L. erythrocarpa*. As shown in Fig. 1D, the activation curves at control, 10, 20, and 100 μg/mL of MeOH extract are shifted to the right according to increases in concentration, while the activation curves at 200 and 300 μg/mL MeOH extract basically overlapped. The $V_{1/2}$ calculations were consistent with this finding, yielding values of -15.2±0.42, -14.2±0.28, -8.36±0.35, 3.21±0.69, 1.10±0.59, -3.85±1.97, and -2.38±0.83 mV at control, 10, 20, 50, 100, 200 and 300 μg/mL MeOH extract, respectively (n=8). Thus, the $V_{1/2}$ values for experiments run in the presence of 10-100 μg/mL MeOH extract significantly increased according to concentration ($P<0.05$, n=8), whereas those for experiments run in the presence of 200 and 300 μg/mL, relatively high concentrations, are not significantly different from each other ($P>0.05$, n=8). These findings indicate that MeOH extract of *L. erythrocarpa* may change activation gating at 10-100 μg/mL, while those high concentrations such as 200 and 300 μg/mL have induced maximal effects on HERG channel current.

Effect of *L. erythrocarpa* on the activated current-voltage relationship

In addition, the effect of MeOH extract of *L. erythrocarpa* on activated currents was tested. The activated current-voltage relationship was obtained with the use of a voltage-clamp protocol shown at the top of Fig. 2A. A depolarizing pulse to +50 mV, which induced a full activation, was followed by various levels of test pulses. The amplitude of the current was measured at its peak before deactivation occurred, and then the data were normalized to the respective maximal currents in the control. Next, the normalized data were averaged and plotted against the test potential (Fig. 2B). The activated current-voltage relationship showed a typical inward rectification of the HERG channel due to the rapid inactivation. The MeOH extract of *L. erythrocarpa* reduced the current within the wide range of membrane potentials from -140 to +30 mV concentration-dependently. Also, the reversal potentials before and after treatment with 10, 100, and 300 μg/mL MeOH extract were -91.3±1.9, -90.5±2.3 ($P>0.05$, n=9), -85.8±2.4, and -77.5±3.2 mV, respectively ($P<0.05$, n=9). Considering that K^+ channel has relatively high selectivity for the permeating ion, K^+ rather than Na^+, Ca^{2+}, and Cl^-, the MeOH extract at relatively high concentrations of 100 and 300 μg/mL, could perturb the ion-selectivity of HERG channel by inducing non-specific membrane permeabilization or membrane leakage.

Fraction-dependent inhibition of HERG channels by *L. erythrocarpa*

Next, we examined the effect of several solvent fractions of *L. erythrocarpa* on the HERG current by comparing the changes

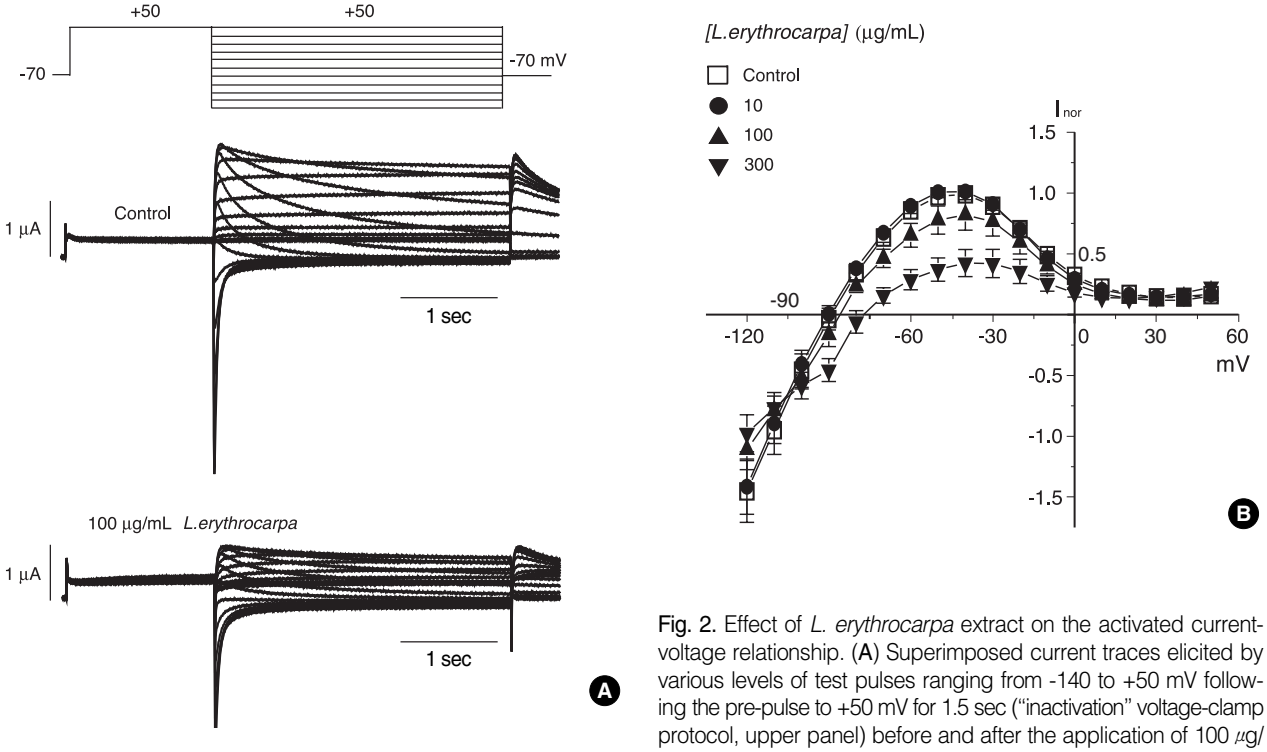

Fig. 2. Effect of *L. erythrocarpa* extract on the activated current-voltage relationship. (**A**) Superimposed current traces elicited by various levels of test pulses ranging from -140 to +50 mV following the pre-pulse to +50 mV for 1.5 sec ("inactivation" voltage-clamp protocol, upper panel) before and after the application of 100 μg/mL *L. erythrocarpa* extract (center and lower panels, respectively). (**B**) The I-V curve is for the maximal repolarization-evoked (tail) outward currents against the repolarization potential. Symbols with error bars represent the means±S.E.M. (n=9).

of I_{HERG} and I_{tail} by each solvent fraction, using the hexane fraction, $CHCl_3$ fraction, EtOAc fraction, BuOH fraction, and H_2O fraction at the same concentrations (100 μg/mL) using the same protocol as Fig. 1, 3A shows an example of a voltage-clamp recording from the *Xenopus* oocyte cell with the representative current traces from a cell in control and after exposure to 100 μg/mL of each solvent fraction. When 100 μg/mL of the hexane fraction, $CHCl_3$ fraction, or EtOAc fraction of *L. erythrocarpa* was added to the perfusate, both I_{HERG} and I_{tail} were suppressed relatively weakly (Fig. 3A, upper and lower panels). In contrast, 100 μg/mL of the BuOH fraction or the H_2O fraction inhibited both I_{HERG} and I_{tail} relatively strongly (Fig. 3A, lower panels). The amplitudes of I_{HERG} and I_{tail} were normalized to the peak amplitude obtained under control conditions and were plotted against the potential of the step depolarization (Fig. 3B, C, respectively). Then, we normalized values in Fig. 3C to the respective maximum value at each fraction to examine possible activation curve shifts induced by fractions of *L. erythrocarpa*. As shown in Fig. 3D, the activation curves in the control oocytes, as well as those treated with the hexane fraction and $CHCl_3$ fraction, basically overlapped, whereas the curves for the EtOAc fraction, BuOH fraction, and H_2O fraction were shifted rightward. The $V_{1/2}$ calculations were consistent with this finding, yielding values of -15.3±0.43, -17.0±0.47, -14.1±0.20, -8.37±0.94, -2.77±2.12, and 0.56±0.64 mV in the control and the

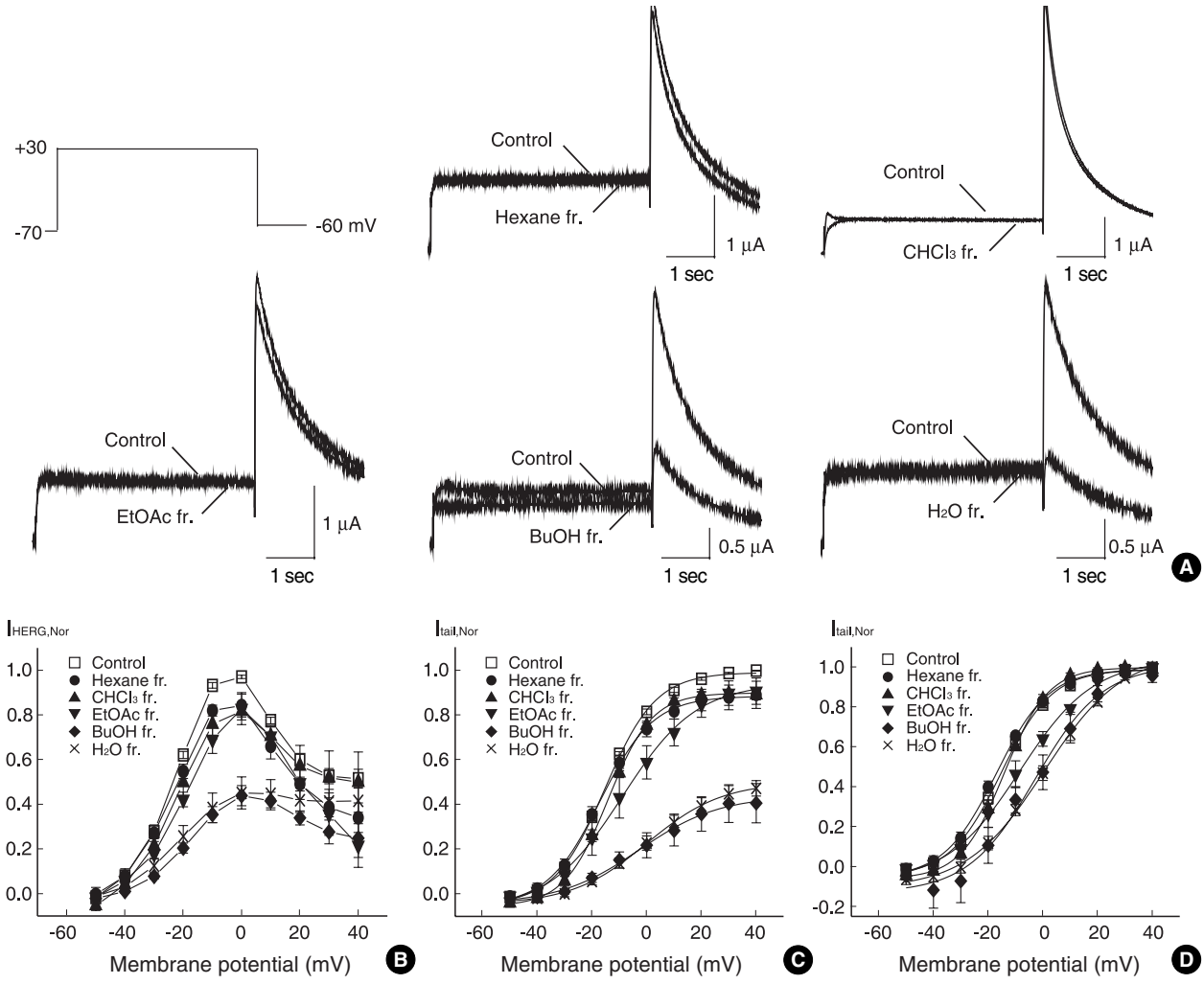

Fig. 3. Effect of different solvent fractions of *L. erythrocarpa* on the HERG current by comparing the changes of I_{HERG} and tail currents with each solvent fraction: the hexane fraction, $CHCl_3$ fraction, EtOAc fraction, BuOH fraction, and H_2O fraction at the same concentrations (100 μg/mL). (A) Superimposed current traces from a cell depolarized to +30 mV before and after exposure to the hexane fraction, $CHCl_3$ fraction, EtOAc fraction, BuOH fraction, and H_2O fraction of *L. erythrocarpa*, respectively. (B) Plot of the HERG current (I_{HERG}) measured at the end of depolarizing pulses against the pulse potential in different solvent fractions of *L. erythrocarpa* (obtained from **A**). (**C**) Plot of the normalized tail current measured at its peak just after repolarization. The amplitude of the tail current in the absence of *L. erythrocarpa* was taken as one. Control data were fitted to the Boltzmann equation, $y=1/\{1+\exp[(-V+V_{1/2})/dx]\}$, with $V_{1/2}$ of -15.3 mV. (**D**) Activation curves with values normalized to the respective maximum value for each fraction of *L. erythrocarpa*. Symbols with error bars represent means±SEM (n=8-22).

hexane fraction, $CHCl_3$ fraction, EtOAc fraction, BuOH fraction and H_2O fraction-treated groups, respectively (n=8-22).

Table 1. Comparison of the effect of different fractions (hexane fraction, $CHCl_3$ fraction, EtOAc fraction, BuOH fraction, and H_2O fraction) of *L. erythrocarpa* on HERG current

Solvent fractions	$V_{1/2}$ (mV)	$V_{1/2}$ shift from control (mV)	G/G_{max}
Control	-15.27±0.43	–	1.00±0.00
Hexane fr.	-17.02±0.47	-3.19±1.86	0.89±0.06
$CHCl_3$ fr.	-14.14±0.20	+2.07±1.03	0.89±0.05
EtOAc fr.	-8.37±0.94	+8.69±1.48*	0.90±0.06
BuOH fr.	-2.77±2.12	+12.72±3.25*	0.40±0.09*
H_2O fr.	+0.56±0.64	+18.06±3.47*	0.47±0.03*

Means±SEM (n=8 for all groups, *P<0.05).
fr., fraction.

These findings indicate that the EtOAc fraction, BuOH fraction, and H_2O fraction of *L. erythrocarpa* may change activation gating at 100 μg/mL.

We then compared the effects of *L. erythrocarpa* fractions on values of $V_{1/2}$, and the g_{max} that is obtained from the maximal amplitude of the I_{tail} curve in Fig. 3C. As shown in Table 1, the BuOH fraction and H_2O fraction changed $V_{1/2}$ significantly (n=8, P<0.05) and decreased g_{max} by 59.6±8.7% and 52.9 ±3.5%, respectively (n=8, P<0.05), while EtOAc fraction changed $V_{1/2}$ significantly (n=8, P<0.05) but did not change g_{max} (n=8, P>0.05).

Effects of H_2O and BuOH fractions on HERG currents

Since the H_2O and BuOH fractions exhibited the strongest

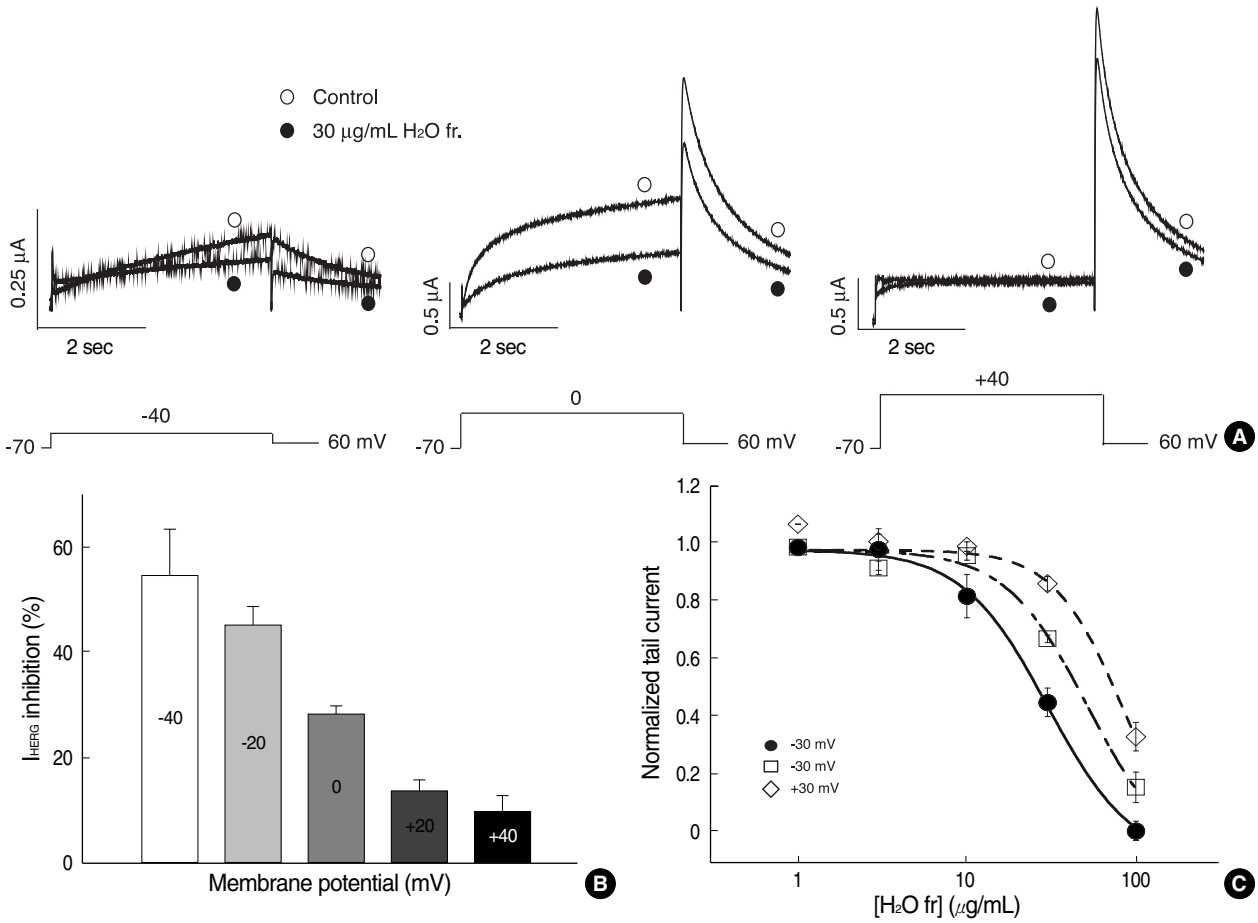

Fig. 4. Voltage dependence of HERG current blocked by the H_2O fraction of *L. erythrocarpa*. (**A**) Current traces from a cell depolarized to -40 mV (left panel), 0 mV (middle panel) and +40 mV (right panel), before and after exposure to 30 μg/mL of the H_2O fraction of *L. erythrocarpa*, showing increased blockade of HERG current at the more negative potential. The protocol consisted of 4-sec depolarizing steps to -40 mV, 0 mV or +40 mV from a holding potential of -70 mV, followed by repolarization to -60 mV. (**B**) HERG current inhibition at different voltages by the H_2O fraction of *L. erythrocarpa*. At each depolarizing voltage step (-40, -20, 0, +20 or +40 mV), the tail currents in the presence of 30 μg/mL H_2O fraction of *L. erythrocarpa* were normalized to the tail current obtained in the absence of *L. erythrocarpa*. Bars with error bars represent means±SEM (n=6). (**C**) Concentration-dependent block of HERG current by the H_2O fraction at different membrane potentials. At each depolarizing voltage step (-30 mV, 0 mV or +30 mV), the tail currents in the presence of various concentrations of the H_2O fraction were normalized to the tail current obtained in the absence of *L. erythrocarpa*, and plotted against H_2O fraction concentrations. Symbols with error bars represent means±SEM (n=6). The line represents the data fits to the Hill equation.

changes in $V_{1/2}$ and g_{max} among the solvent fractions, we first determined whether the effect of the H_2O fraction of *L. erythrocarpa* is voltage dependent by comparing the decrease of I_{tail} induced by the fraction at different potentials (Fig. 4). We found that a higher degree of blockade was present at more negative voltages (Fig. 4A). As shown in Fig. 4B, the I_{tail} inhibition by 30 μg/mL of the H_2O fraction at different voltages (-40, -20, 0, +20, and +40 mV) was 54.8±8.4, 45.3±3.6, 28.4±1.2, 14.0±1.8, and 9.8±2.7%, respectively (n=6, P<0.05). Dose-response relationships were obtained at -30, 0, and +30 mV, and the data were fitted by Hill equations (Fig. 4C), giving IC_{50} values of 30.1±1.13, 51.9±3.87, and 83.0±7.80 μg/mL, and Hill coefficients of 1.72±0.11, 1.78±0.20, and 2.13±0.49 at -30, 0 and +30 mV, respectively (n=6), suggesting that the H_2O fraction-induced blockade of I_{tail} progressively decreases with increasing depolarization. Collectively, these findings indicate that the H_2O fraction of *L. erythrocarpa*-induced blockade of I_{tail} is voltage-dependent.

Next, we found that a higher degree of blockade by the BuOH fraction of *L. erythrocarpa* was also present at more negative voltages (Fig. 5). As shown in Fig. 5B, the I_{tail} inhibition by 30 μg/mL BuOH fraction at different voltages (-40, -20, 0, +20, and +40 mV) was 79.7±8.2, 73.0±10.0, 63.2±10.6, 52.4±10.1, and 46.5±10.2%, respectively (n=6, P<0.05). Dose-response relationships were obtained at -30, 0, and +30 mV, and the data were fitted by Hill equations (Fig. 5C), giving IC_{50} values of 10.4±0.71, 23.4±2.43, and 39.5±7.83 μg/mL, and Hill coefficients of 5.97±10.7, 1.39±0.19, and 1.51±0.42 at -30, 0 and +30 mV, respectively (n=6), suggesting that the BuOH fraction-induced blockade of I_{tail} progressively decreases with increasing depo-

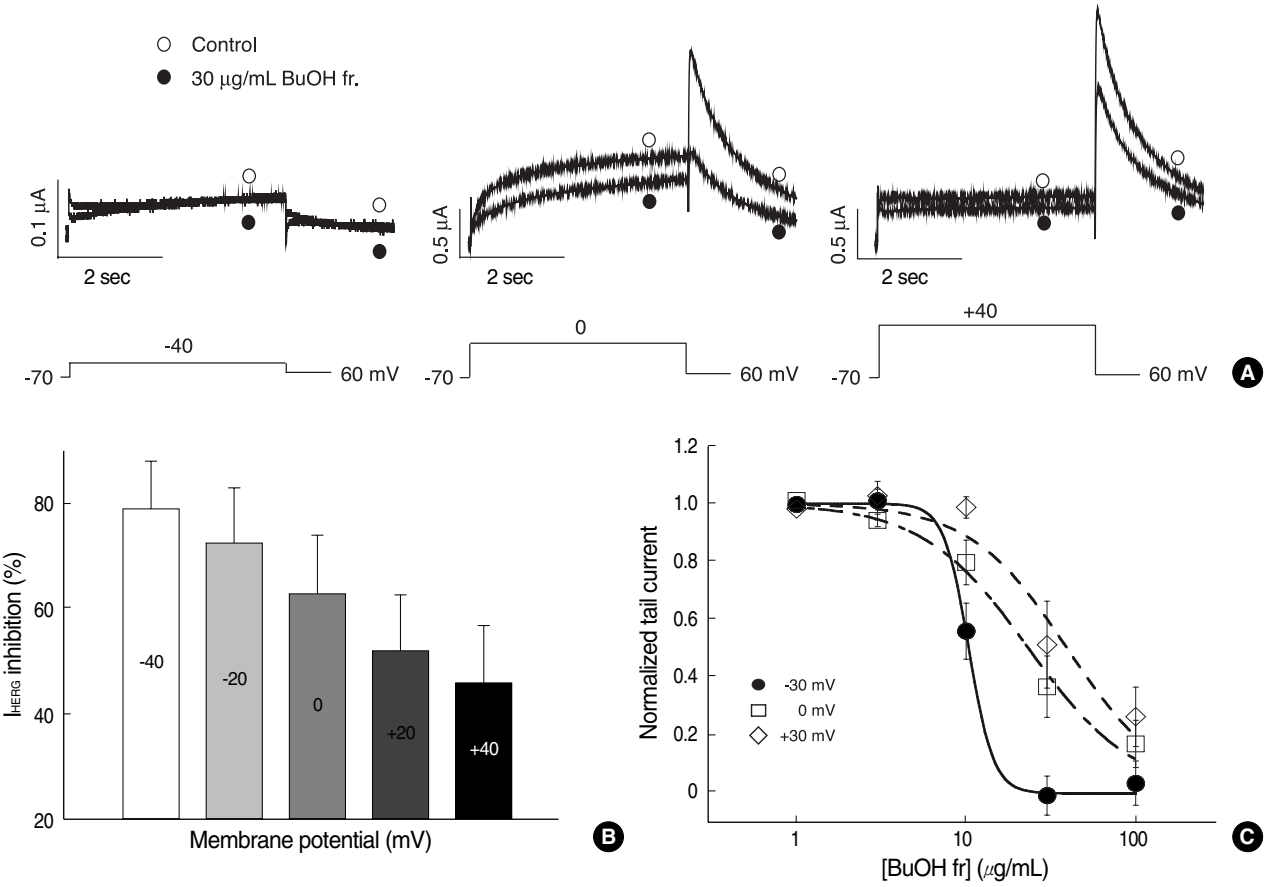

Fig. 5. Voltage dependence of HERG current blocked by the BuOH fraction of *L. erythrocarpa*. (**A**) Current traces from a cell depolarized to -40 mV (left panel), 0 mV (middle panel) and +40 mV (right panel), before and after exposure to 30 μg/mL of the BuOH fraction of *L. erythrocarpa*, showing an increased blockade of HERG current at the more negative potential. The protocol consisted of 4-sec depolarizing steps to -40 mV, 0 mV or +40 mV from a holding potential of -70 mV, followed by repolarization to -60 mV. (**B**) HERG current inhibition at different voltages by the BuOH fraction of *L. erythrocarpa*. At each depolarizing voltage step (-40, -20, 0, +20 or +40 mV), the tail currents in the presence of 30 μg/mL BuOH fraction of *L. erythrocarpa* were normalized to the tail current obtained in the absence of *L. erythrocarpa*. Bars with error bars represent means±SEM (n=6). (**C**) Concentration-dependent block of HERG current by the BuOH fraction at different membrane potentials. At each depolarizing voltage step (-30 mV, 0 mV or +30 mV), the tail currents in the presence of various concentrations of the BuOH fraction were normalized to the tail current obtained in the absence of *L. erythrocarpa*, and plotted against BuOH fraction concentrations. Symbols with error bars represent means±SEM (n=6). The line represents the data fits to the Hill equation.

larization. Collectively, these findings indicate that the BuOH fraction of *L. erythrocarpa*-induced blockade of I_{tail} is voltage-dependent.

Time dependence of HERG channel inhibition by H_2O and BuOH fraction

In addition, we found that the block of HERG currents by H_2O fraction and BuOH fraction of *L. erythrocarpa* showed relatively weak time dependence. We activated currents using a protocol containing a single depolarizing step to 0 mV for 8 sec (Fig. 6A). After obtaining the control measurement, 100 μg/mL of the H_2O fraction was applied while holding the channels in the closed state at -70 mV and the recordings were made. Analysis of the test pulse after H_2O fraction application showed an increase of blocking to 74% at 8 sec in a representative cell (Fig. 6A). The fractional sustained current (obtained by normalizing the currents with H_2O fraction of *L. erythrocarpa* relative to control currents) decreased slightly with ongoing depolarization (Fig. 6B). At the beginning of the pulse, the fractional current was 0.378 ± 0.065 of the control, and it declined slightly to 0.259 ± 0.088 after 1 sec at a test potential of 0 mV (Fig. 6B; n=5). These findings indicate that HERG channels are greatly blocked by H_2O fraction of *L. erythrocarpa* at the holding potential. Similar to the results obtained from the H_2O fraction, the BuOH fraction of *L. erythrocarpa* also shows relatively weak time-dependent block of HERG current (Fig. 6C, D). In a representative cell, 100 μg/mL BuOH fraction application showed an increase of blocking to 79% at 8 sec, and the fractional sustained current slightly decreased with ongoing depolarization (Fig. 6C). At the beginning of the pulse, the fractional current was 0.349 ± 0.052 of the control, and it declined slightly to 0.246 ± 0.067 after 1 sec at a test potential of 0 mV (Fig. 6D; n=5). These findings indicate that HERG channels are also greatly blocked by BuOH fraction of *L. erythrocarpa* while remaining at the holding potential.

DISCUSSION

Our results indicate that extracts of *L. erythrocarpa* is an inhibitor of HERG channels. The IC_{50} values of *L. erythrocarpa* were -50 μg/mL (at +40 mV) for HERG channels heterologously expressed in Xenopus oocytes. Due to the specific properties of the *Xenopus* oocyte expression system, such as the vitelline membrane and egg yolk, higher extracellular concentrations of the drug are required to block HERG chan-

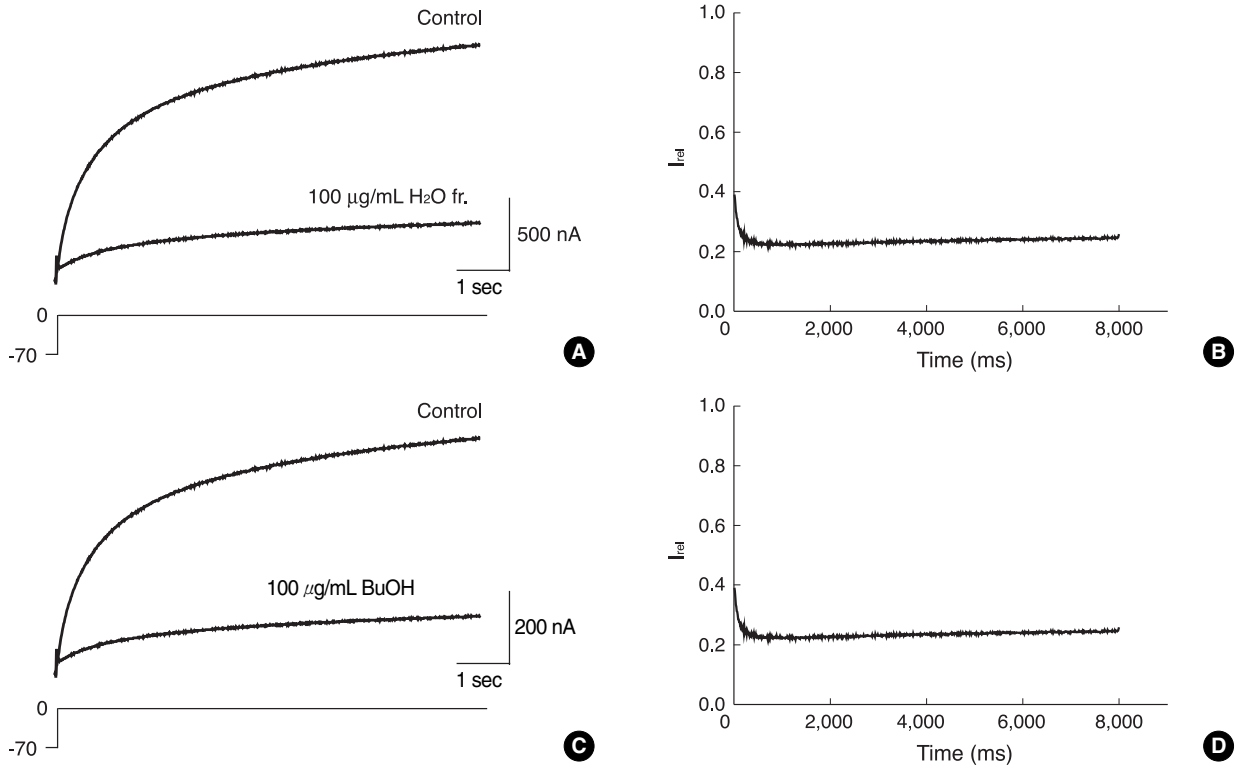

Fig. 6. Relative change in sustained HERG currents in response to H_2O or BuOH fractions of *L. erythrocarpa*. (**A**, **C**) Original recording of currents under control conditions (Control) and in the presence of H_2O (**A**) or BuOH (**C**) fraction of *L. erythrocarpa* (100 μg/mL each) during voltage steps to 0 mV. After having recorded the control measurement, the oocyte was clamped at -70 mV for 13 min during superfusion with the each fraction. (**B**, **D**) Relative current (I_{rel}) obtained by dividing the H_2O (**C**) or BuOH (**D**) fraction current by the control currents of the recording in **A** or **C**, respectively. Time 0 ms corresponds to the beginning of the depolarizing voltage step.

nels than to inhibit native I_{Kr} in mammalian cells (14, 15).

It has been shown that various K^+ currents are associated with the proliferation of cancer cells. Ca^{2+}-activated K^+ channels has been shown to play a role in the physiological regulation during proliferation of human prostate, neuroblastoma or medulloblastoma cancer cells (16-18). The delayed rectifier K^+ currents (I_K) have been shown to correlated with mitogenesis and to constitute an link between cytokines activated signaling cascade and cell cycle (19, 20). HERG has been found abundantly expressed in a variety of tumor cells of different histogenesis where it plays a crucial role in the development and maintenance of their neoplastic phenotype (21). The high frequency of expression of HERG in primary human endometrial cancers, as compared to normal and hyperplastic endometrium, has candidated this protein as a potential marker of cancerous versus hyperplastic endometrial growth (10). Several models have been proposed to explain the involvement of K^+ channels in mitogenesis. Cone and Tonigier have suggested that K^+ channel activity would determine a shift in the resting membrane potential of cells, this latter event being mitogenic (22). Since the fruit and leaves of *L. erythrocarpa* show anti-tumor activity (4, 5), our results suggest that *L. erythrocarpa*-induced block of the HERG channel could change the resting membrane potential, which may contribute to the anti-tumor effects in various cancer cell lines.

The use of *L. erythrocarpa* as an antimicrobial or anticancer agent has been suggested. It has been shown that the extract from *L. erythrocarpa* showed over 90% antimicrobial activity, according to an in vivo bioassay method (23). Lee et al. reported that methyllinderone, one of the compounds isolated from a EtOAc fraction of *L. erythrocarpa* methanol extract, showed significant cytotoxicity against three cancer cell lines with ED_{50} values of 2.2-8.3 μg/mL (5). Considering that H_2O and BuOH fractions had relatively higher effects on $V_{1/2}$ and g_{max} than EtOAc fraction, compounds other than methyllinderone could block the HERG channel.

HERG channel blockers have been shown to inhibit the channels in a voltage-dependent manner, suggesting that these drugs bind to the open or inactivated state of HERG channels. For example, haloperidol, an antipsychotic drug (24), and two histamine receptor antagonists, terfenadine and astemizole (25), have been found to preferentially bind to the inactivated state of HERG, whereas the gastrointestinal prokinetic agent cisapride has been shown to block the channel in its open state (26). We have shown here that the amplitudes of maximum I_{HERG} and the maximum I_{tail} were decreased by *L. erythrocarpa* extract, and the blockade of I_{tail} magnitude by BuOH and H_2O fractions increased with more negative voltages, which decrease the open probability and inhibit inactivation. Also, the voltage dependence of the HERG channel blockade by the BuOH (Fig. 5) and H_2O fractions (Fig. 4) indicate that this drug preferentially blocks HERG channels in the closed state rather than either the open or inactivated states. Consistent results were that *L. erythrocarpa* blocks HERG channel at the holding potential rather than at the depolarizing pulse (Fig. 6). Considering that the $V_{1/2}$ values of activation curves in the absence and presence of 10-100 μg/mL *L. erythrocarpa* extract significantly increased according to concentration, our findings suggest that *L. erythrocarpa* blocks closed state HERG channels and concomitantly changes activation gating. In addition, the shift in $V_{1/2}$ and the reduction in g_{max} were greatly affected by the BuOH and H_2O fractions rather than the hexane fraction, $CHCl_3$ fraction, or EtOAc fraction (Fig. 3, Table 1). This finding suggested that the active ingredients inhibiting HERG channel should be included in more polar solvent than non-polar solvent.

Shifting of the voltage dependence of activation (Fig. 1D) by positively charged molecule could be considered to be a general phenomenon caused by a non-specific surface charge effect (27, 28). This effect is thought to reflect the binding of the molecule to diffuse or aggregate negatively charged moieties near the outer mouth of the channels, altering the voltage field that is sensed by the channel gating mechanism. According to this hypothesis, current activation and deactivation should be affected to the same extent by *L. erythrocarpa*. However, there was a larger increase of activation time constant than the decrease of deactivation time constant (n=3, data not shown). In addition, the g_{max} of HERG channels (current magnitude at highly depolarized potentials where there is already a high probability of opening) was significantly reduced by *L. erythrocarpa* (Fig. 1C), which cannot be explained by the surface charge theory. Therefore, we excluded the surface charge theory as a main mechanism of the *L. erythrocarpa* effect.

There are several studies showing the effect of *Lindera* species (Lauraceae) on K^+ channels. Wang et al. (29) suggested that the cardioprotective effect by *L. strychnifolia* was due to the opening of the mitochondrial K_{ATP} channels in cardiac myocytes, because the improvement of myocardial dysfunction after global ischemia by *L. strychnifolia* was completely abolished by pre-treatment with a mitochondrial K_{ATP} channel blocker, 5-HD. In rat isolated ventricular myocytes, dicentrine, an aporphine alkaloid isolated from the root of *L. megaphylla*, prolongs the APD_{50} and reduces the rate of action potential upstroke, indicating that dicentrine may possess antiarrhythmic activity (30). Also, it has been shown that the IK in guinea pig ventricular myocytes was inhibited by dicentrine, with IC_{50} values between 3 and 10 μM (30). Although it has not been reported that *L. erythrocarpa* prolongs the APD or induces cardiac arrhythmia to our knowledge, our results suggest that *L. erythrocarpa* blocks the HERG channel, a major component of the I_{Kr}, which could make the heart prone to arrhythmia since I_{Kr} is one of the targets for antiarrhythmic therapy and the blocking of this current is expected to increase the APD and thereby increase the refractory period (7).

In conclusion, we have shown here that *L. erythrocarpa* blocks HERG channel, resulting in a shift of voltage-dependence of channel activation and reduction of g_{max}, and that the H_2O

and BuOH fractions exhibits the strongest changes in $V_{1/2}$ and g_{max} among the solvent fractions. Considering that *L. erythrocarpa* have been used as a folk medicine and shows anticancer activity and that HERG channel is important target regulating proliferation of the tumor cells and determining cardiac APD, our results could explain the anticancer effect and potentially arrhythmogenic effect of *L. erythrocarpa*.

REFERENCES

1. Sun BY, Chung YH. *Monbographic study of the Lauracea in Korea. Kor J Plant Tax 1988; 18: 133-51.*
2. Liu SY, Hisada S, Inagaki I. *Terpenses of Lindera erythrocarpa. Phytochemistry 1973; 12: 233.*
3. Liu SY, Hisada S, Inagaki I. *Constituents of Lindera erythrocarpa. Phytochemistry 1973; 12: 472.*
4. Oh HM, Choi SK, Lee JM, Lee SK, Kim HY, Han DC, Kim HM, Son KH, Kwon BM. *Cyclopentenediones, inhibitors of farnesyl protein transferase and anti-tumor compounds, isolated from the fruit of Lindera erythrocarpa Makino. Bioorg Med Chem 2005; 13: 6182-7.*
5. Lee SM, Baek SH, Lee CH, Lee HB, Kho YH. *Cytotoxicity of Lignans from Lindera erythrocarpa Makino. Nat Prod Sci 2002; 8: 100-2.*
6. Sanguinetti MC, Jurkiewicz NK. *Two components of cardiac delayed rectifier K^+ current. Differential sensitivity to block by class III antiarrhythmic agents. J Gen Physiol 1990; 96: 195-215.*
7. Spector PS, Curran ME, Zou A, Keating MT, Sanguinetti MC. *Fast inactivation causes rectification of the IKr channel. J Gen Physiol 1996; 107: 611-9.*
8. Curran ME, Splawski I, Timothy KW, Vincent GM, Green ED, Keating MT. *A molecular basis for cardiac arrhythmia: HERG mutations cause long QT syndrome. Cell 1995; 80: 795-803.*
9. Bianchi L, Wible B, Arcangeli A, Taglialatela M, Morra F, Castaldo P, Crociani O, Rosati B, Faravelli L, Olivotto M, Wanke E. *Herg encodes a K+ current highly conserved in tumors of different histogenesis: a selective advantage for cancer cells? Cancer Res 1998; 58: 815-22.*
10. Cherubini A, Taddei GL, Crociani O, Paglierani M, Buccoliero AM, Fontana L, Noci I, Borri P, Borrani E, Giachi M, Becchetti A, Rosati B, Wanke E, Olivotto M, Arcangeli A. *HERG potassium channels are more frequently expressed in human endometrial cancer as compared to non-cancerous endometrium. Br J Cancer 2000; 83: 1722-9.*
11. Pardo LA, del Camino D, Sánchez A, Alves F, Brüggemann A, Beckh S, Stühmer W. *Oncogenic potential of EAG K(+) channels. EMBO J 1999; 18: 5540-7.*
12. Suzuki T, Takimoto K. *Selective expression of HERG and Kv2 channels influences proliferation of uterine cancer cells. Inter J Oncol 2004; 25: 153-9.*
13. Sanguinetti MC, Jiang C, Curran ME, Keating MT. *A mechanistic link between an inherited and an acquired cardiac arrhythmia: HERG encodes the IKr potassium channel. Cell 1995; 81: 299-307.*
14. Kiehn J, Lacerda AE, Wible B, Brown AM. *Molecular physiology and pharmacology of HERG. Single-channel currents and block by dofetilide. Circulation 1996; 94: 2572-9.*
15. Thomas D, Wendt-Nordahl G, Rockl K, Ficker E, Brown AM, Kiehn J. *High-affinity blockade of human ether-a-go-go-related gene human cardiac potassium channels by the novel antiarrhythmic drug BRL-32872. J Pharmacol Exp Ther 2001; 297: 753-61.*
16. Parihar AS, Coghlan MJ, Gopalakrishnan M, Shieh CC. *Effects of intermediate-conductance Ca2+-activated K+ channel modulators on human prostate cancer cell proliferation. Eur J Pharmacol 2003; 471: 157-64.*
17. Inglis V, Karpinski E, Benishin C. *Gamma-dendrotoxin blocks large conductance Ca2+-activated K+ channels in neuroblastoma cells. Life Sci 2003; 73: 2291-305.*
18. Carignani C, Roncarati R, Rimini R, Terstappen GC. *Pharmacological and molecular characterisation of SK3 channels in the TE671 human medulloblastoma cell line. Brain Res 2002; 939: 11-8.*
19. Wu H, Wu K, Han Y, Shi Y, Yao L, Wang J, Fan D. *Delayed rectifier K(+) channel regulated by cyclooxygenase-2 in human gastric cancer cell. Zhonghua Zhong Liu Za Zhi 2002; 24: 440-3.*
20. Soliven B, Ma L, Bae H, Attali B, Sobko A, Iwase T. *PDGF upregulates delayed rectifier via Src family kinases and sphingosine kinase in oligodendroglial progenitors. Am J Physiol Cell Physiol 2003; 284: C85-93.*
21. Wang H, Zhang Y, Cao L, Han H, Wang J, Yang B, Nattel S, Wang Z. *HERG K+ channel, a regulator of tumor cell apoptosis and proliferation. Cancer Res 2002; 62: 4843-8.*
22. Cone CD Jr, Tongier M Jr. *Control of somatic cell mitosis by simulated changes in the transmembrane potential level. Oncology 1971; 25: 168-82.*
23. Rim YS, Park YM, Park MS, Kim KY, Kim MJ, Choi YH. *Screening of antioxidants and antimicrobial activity in native plants. Korean J Med Crop Sci 2000; 8: 342-50.*
24. Suessbrich H, Schonherr R, Heinemann SH, Attali B, Lang F, Busch AE. *The inhibitory effect of the antipsychotic drug haloperidol on HERG potassium channels expressed in Xenopus oocytes. Br J Pharmacol 1997; 120: 968-74.*
25. Suessbrich H, Waldegger S, Lang F, Busch AE. *Blockade of HERG channels expressed in Xenopus oocytes by the histamine receptor antagonists terfenadine and astemizole. FEBS Lett 1996; 385: 77-80.*
26. Rampe D, Roy ML, Dennis A, Brown AM. *A mechanism for the proarrhythmic effects of cisapride (Propulsid): high affinity blockade of the human cardiac potassium channel HERG. FEBS Lett 1997; 417: 28-32.*
27. Green WN, Andersen OS. *Surface charges and ion channel function. Annu Rev Physiol 1991; 53: 341-59.*
28. Hille B. *Ionic channels of excitable membranes. 2nd ed. Sunderland, Mass: Sinauer Associates Inc 1992; 459-61.*
29. Wang N, Minatoguchi S, Arai M, Uno Y, Hashimoto K, Xue-Hai C, Fukuda K, Akao S, Takemura G, Fujiwara H. *Lindera strychnifolia is protective against post-ischemic myocardial dysfunction through scavenging hydroxyl radicals and opening the mitochondrial KATP channels in isolated rat hearts. Am J Chin Med 2004; 32: 587-98.*
30. Su MJ, Nieh YC, Huang HW, Chen CC. *Dicentrine, an alpha-adrenoceptor antagonist with sodium and potassium channel blocking activities. Naunyn-Schmiedebergs Arch Pharmacol 1994; 349: 42-9.*